AIP | Applied Physics Letters

Lateral buckling and mechanical stretchability of fractal interconnects partially bonded onto an elastomeric substrate

Haoran Fu, Sheng Xu, Renxiao Xu, Jianqun Jiang, Yihui Zhang, John A. Rogers, and Yonggang Huang

Citation: Applied Physics Letters **106**, 091902 (2015); doi: 10.1063/1.4913848
View online: http://dx.doi.org/10.1063/1.4913848
View Table of Contents: http://scitation.aip.org/content/aip/journal/apl/106/9?ver=pdfcov
Published by the AIP Publishing

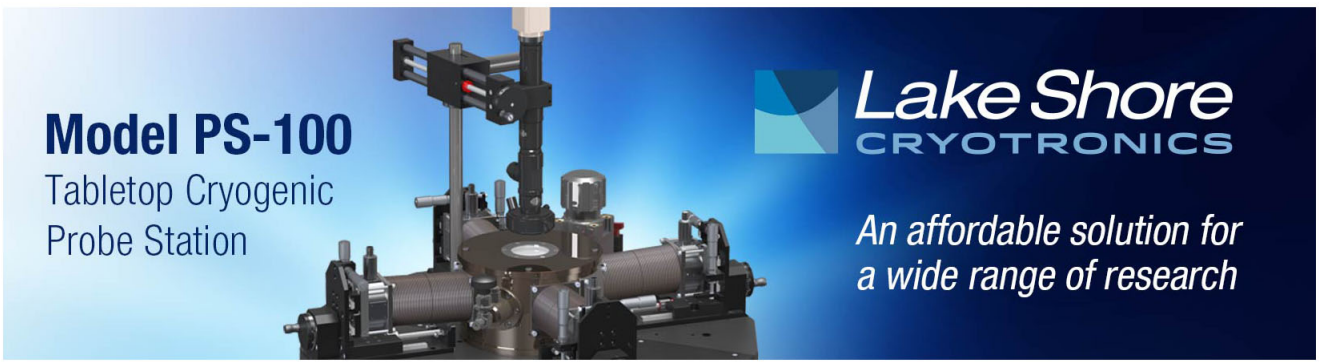

Lateral buckling and mechanical stretchability of fractal interconnects partially bonded onto an elastomeric substrate

Haoran Fu,[1,2] Sheng Xu,[3] Renxiao Xu,[2] Jianqun Jiang,[1] Yihui Zhang,[2,4] John A. Rogers,[3,a)] and Yonggang Huang[2,a)]
[1]*Department of Civil Engineering and Architecture, Zhejiang University, Hangzhou 310058, China*
[2]*Departments of Civil and Environmental Engineering and Mechanical Engineering; Center for Engineering and Health; Skin Disease Research Center, Northwestern University, Evanston, Illinois 60208, USA*
[3]*Department of Materials Science and Engineering; Frederick Seitz Materials Research Laboratory; University of Illinois at Urbana-Champaign, Urbana, Illinois 61801, USA*
[4]*Center for Mechanics and Materials, Tsinghua University, Beijing 100084, China*

(Received 29 January 2015; accepted 18 February 2015; published online 2 March 2015)

Fractal-inspired designs for interconnects that join rigid, functional devices can ensure mechanical integrity in stretchable electronic systems under extreme deformations. The bonding configuration of such interconnects with the elastomer substrate is crucial to the resulting deformation modes, and therefore the stretchability of the entire system. In this study, both theoretical and experimental analyses are performed for postbuckling of fractal serpentine interconnects partially bonded to the substrate. The deformation behaviors and the elastic stretchability of such systems are systematically explored, and compared to counterparts that are not bonded at all to the substrate. [http://dx.doi.org/10.1063/1.4913848]

Recent research in stretchable/flexible electronics[1–10] and optoelectronics[11–14] demonstrates the possibility for rendering conventionally rigid and brittle high-performance inorganic semiconductors in forms that can provide elastic responses to extremely large levels of deformation. The superior mechanical attributes open up many important application opportunities that cannot be addressed with established technologies, including, eye-ball like digital cameras,[15–17] soft surgical instruments,[18–21] "epidermal" health/wellness monitors,[22–28] and electronic sensors for robotics.[29–33] One of the strategies utilized to achieve stretchable mechanics is the island-bridge design,[15,23,34–37] where the active components of the device (i.e., islands) are integrated with elastomeric substrates, and joined by deformable interconnects (i.e., bridges). In this design, the deformable interconnects can be made either in non-bonded formats, or partially or fully bonded to the elastomeric substrates, depending on the specific requirements of the applications. Interconnects that are fully non-bonded usually offer the highest stretchabilities because of the minimum mechanical constraints imposed by the substrate. The mechanical behaviors of such cases have been explored in several recent reports.[32,38–42] Typically, surface microstructures[40] on the elastomeric substrate (e.g., textured surface in pyramidal configuration with raised support posts) are required to reduce the adhesion with the deformable interconnects and to enable their freestanding deformations.[34,38] Interconnects fully bonded onto the substrate can be achieved relatively easily using traditional integration schemes. Here, the deformation mechanisms depend strongly on constraints imposed by the substrate.[23,26,43–46] Interconnects partially bonded to the substrate exhibit different buckling modes and levels of stretchability from either of these other two cases. Although the mechanical behaviors in such systems and the quantitative relationship between the stretchability and various geometrical parameters are also critically important to practical applications, systematic studies have not been performed. The work reported here involves examination of the buckling behaviors of partially bonded interconnects through combined experimental measurements and finite element analyses (FEA). One result is a simplified model for device stretchability that can be useful in optimizing the designs of the interconnects.

Our focus is an island-bridge structure with the interconnect constructed in a 2nd order fractal serpentine configuration.[37,41] The 1st order interconnect consists of straight wires and half circles that are joined in series, as shown in the left panel of Fig. 1(a). The 2nd order interconnect, shown in the right panel of Fig. 1(a), is created by reducing the scale of the 1st order interconnects, followed by 90° rotation, and then connecting them to reproduce the layout of the original geometry. Let $\eta^{(i)}$ denote the height/spacing aspect ratio at ith order ($i = 1,2$), and then the height $h^{(i)}$ can be related to the spacing $l^{(i)}$ by $h^{(i)} = \eta^{(i)} l^{(i)}$. The height $h^{(2)}$ is also related to the spacing $l^{(1)}$ by the number of unit cells m (Fig. 1(b)) as $h^{(2)} = 2ml^{(1)}$. The spacing and height at each order are then scaled with the spacing ($l^{(2)}$) of the 2nd order by

$$l^{(1)} = \frac{\eta^{(2)}}{2m} l^{(2)}, \quad h^{(1)} = \frac{\eta^{(1)}\eta^{(2)}}{2m} l^{(2)}, \quad h^{(2)} = \eta^{(2)} l^{(2)}. \quad (1)$$

It shows that the geometry of 2nd order serpentine structure is characterized by one base length ($l^{(2)}$) and three non-dimensional parameters, namely, the height/spacing ratio ($\eta^{(1)}, \eta^{(2)}$) and number (m) of unit cell. To achieve a high surface filling ratio in application, $\eta^{(1)}$ and $\eta^{(2)}$ are usually different from each other.[37]

Experiments on fully non-bonded and partially bonded fractal serpentine interconnects were performed to investigate

a)Authors to whom correspondence should be addressed. Electronic addresses: y-huang@northwestern.edu and jrogers@illinois.edu.

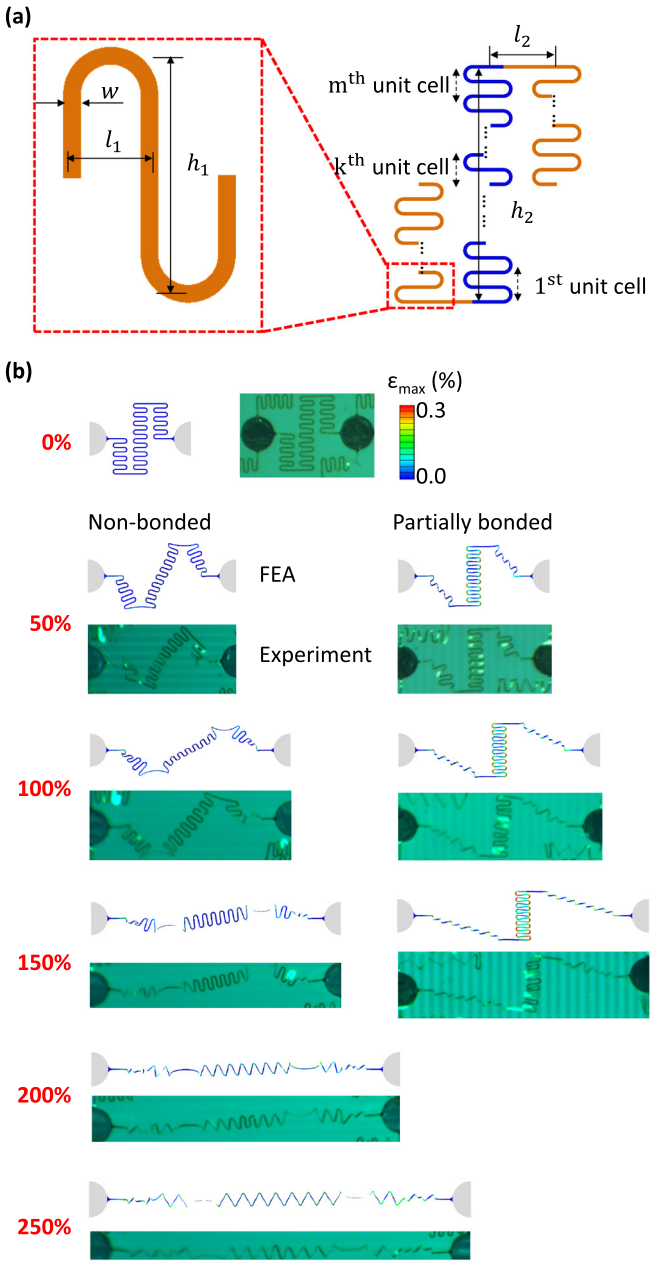

FIG. 1. (a) Illustration of geometric parameters for a second order fractal serpentine interconnect with m unit cells. (b) Optical images and corresponding FEA results of deformed configurations for the interconnects non-bonded (left column) and partially (right column) bonded to the substrate, under various levels of applied tensile strain.

the different buckling behaviors. The interconnects in test samples consisted of multilayer materials in stacked designs [PI (1.2 μm)/Al (0.6 μm)/PI (1.2 μm), where PI denotes polyimide]. The substrate we used was silicone (Ecoflex, Smooth-On). To enable non-bonded interconnects, the substrate was lubricated using water. For the partially bonded sample, the substrate was unprocessed, and therefore, interconnects were partially bonded to the silicone substrate due to native surface tackiness. In all of the cases, the islands were fully bonded with UV/ozone photochemical process. Mechanical testing was performed with customized uniaxial stretchers, and images of the deformed interconnects were collected with a digital single-lens reflex camera.

Computational models of postbuckling analyses were developed using FEA for both the non-bonded and partially bonded systems. Linear critical buckling analyses were carried out first, and the calculated first order buckling mode was then implemented as an initial geometric defect in the postbuckling analyses. Refined meshes were adopted to ensure accuracy, with the 8-node solid element (C3D8R) and 4-node shell element (S4R) used for the substrate and interconnects, respectively. The circular pads (islands) are joined by interconnects in both systems, and the middle string of the partially delaminated interconnect (the blue part of interconnect in Fig. 1(a)) was bonded to the substrate. The elastic stretchability (referred to as stretchability in the following, for simplicity), as defined by the yield strain (~0.3%), can be then determined.

Fig. 1(b) demonstrates both the experimental images and numerical results on the evolution of deformations in the interconnects under two different bonding conditions. For the non-bonded interconnect on the left panel, the entire structure bends and twists without any evident coupling to the substrate during the postbuckling process. In this case, the interconnect could endure stretching up to ~277% before plastic yielding. The partially bonded interconnect on the right panel experiences a different deformation mode, in which the middle string of the interconnect is highly constrained by the substrate. The resulting stretchability (for reversible deformation) is reduced to ~136%.

We then analyze the influence of geometric parameters on the stretchability for both the non-bonded and partially bonded systems. Various combinations of non-dimensional parameters $(\eta^{(1)}, \eta^{(2)}, m)$ were considered, for a fixed spacing and cross-section of the interconnect, i.e., $(l^{(2)}, w, t_{Al}, t_{PI}) = (1\,\text{mm}, 0.03\,\text{mm}, 0.6\ \mu\text{m}, 1.2\ \mu\text{m})$. As shown in Fig. 2(a), for a fixed 2nd order height/spacing ratio $\eta^{(2)}$, the stretchabilities of both systems increase with increase in the 1st order height/spacing ratio $\eta^{(1)}$ and unit cell number m, while their corresponding ratio approaches a constant (~0.5) for $\eta^{(1)} \geq 3$ (Fig. 2(b)). A feasible explanation is that the length of the middle string of interconnect that adheres to the substrate is nearly half of the total length, and the bonded segment (i.e., middle string) of interconnect poses additional constraints to the rotational deformation of the delaminated segment, as compared to the case of non-bonded system. Such constraints reduce with the increase of $\eta^{(1)}$, since the ratio of vertical distance between the two ends of the delaminated segment in the fully extended state to its horizontal distance decreases gradually. Figs. 2(c) and 2(d) show a similar trend of stretchability versus the 2nd order height/spacing ratio $\eta^{(2)}$, for fixed 1st order height/spacing ratio $\eta^{(1)}$ and unit cell number m.

As the relationship between stretchability and height/spacing ratio is nearly linear when $\eta^{(1)} \geq 3$ and $\eta^{(2)} \geq 3$, a simplified scaling law can be summarized in this regime. Assuming that the stretchability is linearly dependent on the ratio (α) of total wire length (L) to the span (i.e., $2l_2$) of the 2nd order serpentine structure, i.e.,

$$\alpha = \frac{L}{2l_2} = \eta^{(1)}\eta^{(2)} + \frac{(\pi - 2)}{2}\eta^{(2)} + 1, \qquad (2)$$

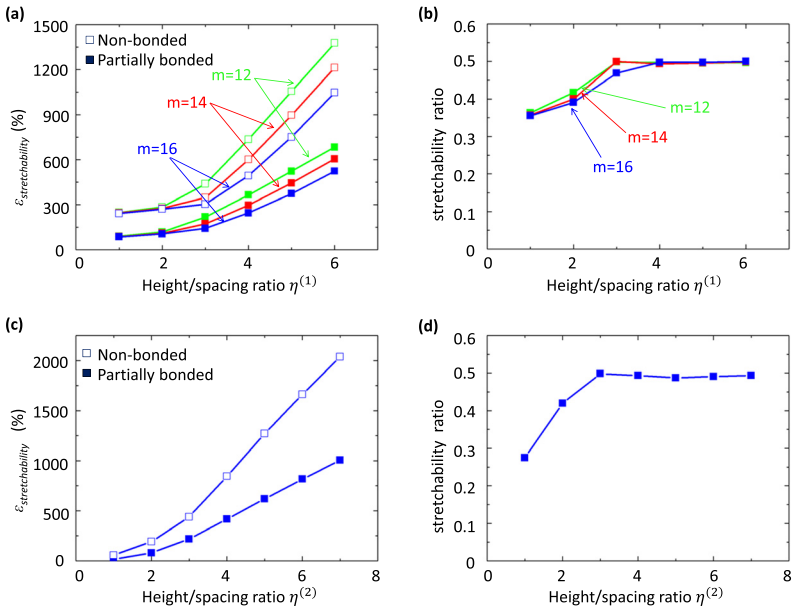

FIG. 2. (a) Stretchability ($\varepsilon_{stretchability}$) of non-bonded and partially bonded interconnects versus height/spacing ratio ($\eta^{(1)}$) for three different number (m) of unit cells, and a fixed $\eta^{(2)} = 3$. (b) Ratio of $\varepsilon_{stretchability}$ for partially bonded interconnects to that for non-bonded interconnects versus height/spacing ratio ($\eta^{(1)}$) for three different number (m) of unit cells, and a fixed $\eta^{(2)} = 3$. (c) Stretchability ($\varepsilon_{stretchability}$) of non-bonded and partially bonded interconnects versus height/spacing ratio ($\eta^{(2)}$) for a fixed $\eta^{(1)} = 3$ and $m = 12$. (d) Ratio of $\varepsilon_{stretchability}$ for partially bonded interconnects to that for non-bonded interconnects versus height/spacing ratio ($\eta^{(2)}$) for a fixed $\eta^{(1)} = 3$ and $m = 12$.

and considering that the increase of m would lead to reduction in the stretchability, due to the decreased rounding radius of half circles that makes the structure harder to bend and twist, the stretchability can be expressed as

$$\varepsilon = F_1[2\eta^{(1)}\eta^{(2)} + (\pi - 2)\eta^{(2)} + 2] + F_2 m, \tag{3}$$

where F_1 and F_2 are non-dimensional functions dependent on the interconnect width w and thickness t. Through multiple linear regression for ε and $(\eta^{(1)}, \eta^{(2)}, m)$, the value of (F_1, F_2) can be determined as (53.5, −66.9) for $(w, t_{Al}, t_{PI}) = (0.03\,\text{mm}, 0.6\ \mu\text{m}, 1.2\ \mu\text{m})$ as adopted herein. The results based on Eq. (3) agree reasonably well with the FEA in Fig. 3. Note that the linear dependence of stretchability on the 1st order height/spacing ratio of the 2nd serpentine structure is similar to the trend reported in the 1st order serpentine structure.[40]

Based on the above results, we are able to optimize the island-bridge structure design for both non-bonded and partially bonded system to achieve simultaneously high surface filling ratio of active device (islands) and large stretchability of entire system. A high areal coverage demands small spacing between two neighboring island, while a large stretchability requires large spacing to accommodate long interconnects. The relationship between the stretchability and the filling ratio (f) is given by

$$\varepsilon_{stretchability}^{system} = \varepsilon_{stretchability}^{interconnnect}(1 - \sqrt{f}), \tag{4}$$

where $\varepsilon_{stretchability}^{system}$ stands for the stretchability of system and $\varepsilon_{stretchability}^{interconnnect}$ denotes the stretchability of interconnect. It is noteworthy that previous designs based on the buckling of straight or conventional serpentine interconnects could yield only ~30% system-level stretchability if the filling ratio reaches 50%. The fractal serpentine structure can resolve this issue due to its space-filling nature.

For an island-bridge design with square-shaped device in a representative size $H = 1$ mm and filling ratio of 50% (Fig. 4(a)), due to the limitations of conventional fabrication

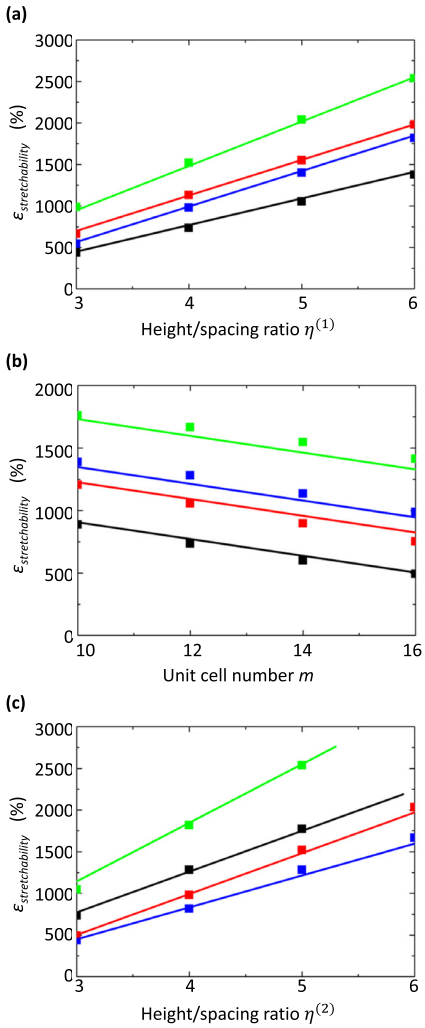

FIG. 3. (a) Results of simplified model and FEA for the stretchability of free-standing serpentine structures versus height/spacing ratio ($\eta^{(1)}$). (b) Results of simplified model and FEA for the stretchability of free-standing serpentine structures versus height/spacing ratio ($\eta^{(2)}$). (c) Results of simplified model and FEA for the stretchability of free-standing serpentine structures versus the number (m) of unit cell. In (a)–(c), the lines all denote results of simplified analytic model, and the square symbols denote FEA results.

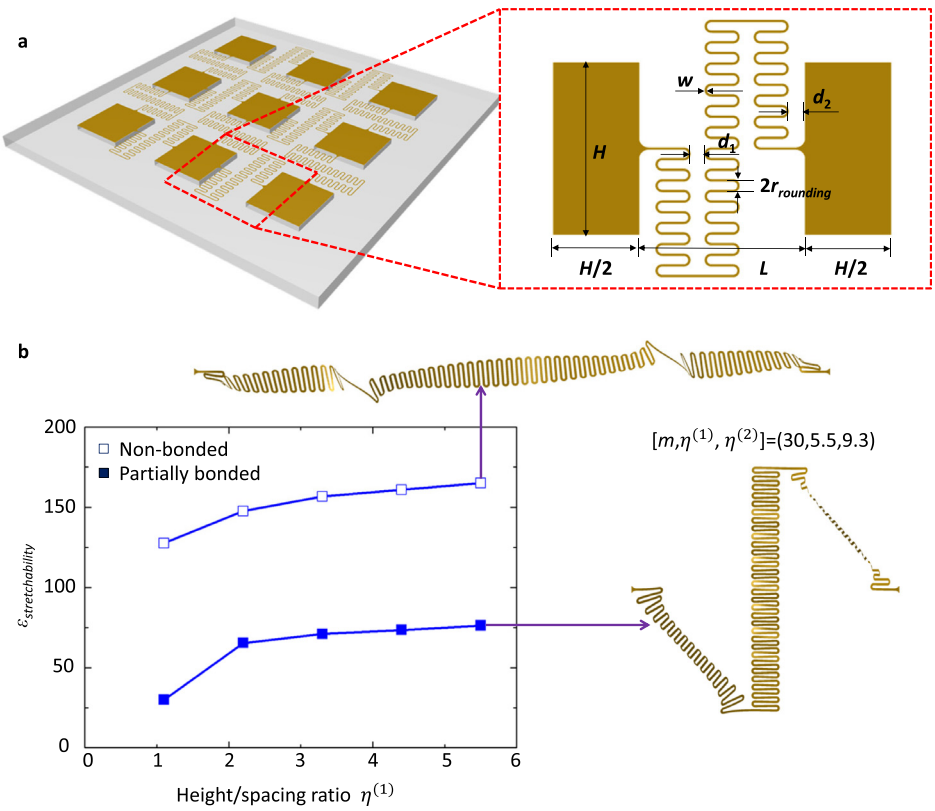

FIG. 4. Design optimization of the 2nd order serpentine interconnects in an island–bridge structure. (a) Schematic of a 3 by 3 array of island–bridge structure, and illustration on the geometric parameters. (b) Maximum stretchability versus the height/spacing ratio ($\eta^{(1)}$) for different number (m) of unit cells (left bottom panel), and the optimized configurations (right bottom panel and top panel) when stretched to the corresponding stretchabilities.

technologies, there are usually some constraints on the geometric parameters, e.g., the width $w \geq 10\,\mu$m, rounding radius $r_{rounding} \geq 10\,\mu$m, the distance between neighboring arcs $d_1 \geq 10\,\mu$m, and the distance between interconnect and island $d_2 \geq 10\,\mu$m. The other parameters are then optimized to achieve the largest stretchability, given that the interconnects do not self-overlap during the deformation. Fig. 4(b) shows that the stretchability increases with the increase in the 1st order height/spacing ratio $\eta^{(1)}$, in which the unit cell number m varies with $\eta^{(1)}$ to fill the whole spacing between the islands. The optimal design shown in the right panel can reach ~165% stretchability of the system for non-bonded system and ~76% for partially bonded system, which are larger than the previous designs using wavy interconnects enabled by Euler buckling of straight wires or conventional serpentine interconnects. It is noteworthy that in practical applications, the electronic system could potentially experience excessive stretching (e.g., with the applied strain larger than the designed elastic stretchability), thereby leading to plastic yielding in the metal layer. When the system is subject to repetitive stretching to a similar extent, irreversible deformations would be accumulated in the interconnects. This could cause the fractal structures to be entangled and/or disordered in the non-bonded constructions, especially in the layout with high densities of islands and interconnects. To avoid this issue, it could be useful to introduce a safety factor for the system-level elastic stretchability in the practical designs.

In summary, this study develops a simplified model of postbuckling analysis for partially bonded fractal serpentine interconnects. Compared with the non-bonded interconnects, the partially bonded serpentine interconnect has a quite different deformation mode. The resulting stretchability approaches half that of the non-bonded interconnects, when the height/spacing ratio for each order is larger than ~3. A design optimization is performed for the stretchable electronics systems with relatively large areal coverage (e.g., 50%) of active devices, to yield an optimal system-level stretchability (e.g., ~165% for non-bonded system, and ~76% for partially bonded system). These results are useful for the biomedical applications of stretchable electronics such as electronic eyeball cameras and epidermal photonic devices.

Y.H. and J.A.R. acknowledge the support from the NSF (DMR-1121262, CMMI-1300846, and CMMI-1400169).

[1]S. P. Lacour, J. Jones, S. Wagner, T. Li, and Z. Suo, Proc. IEEE **93**, 1459 (2005).
[2]D. Y. Khang, H. Jiang, Y. Huang, and J. A. Rogers, Science **311**, 208 (2006).
[3]S. P. Lacour, S. Wagner, R. J. Narayan, T. Li, and Z. Suo, J. Appl. Phys. **100**, 014913 (2006).
[4]H. Jiang, D. Y. Khang, J. Song, Y. Sun, Y. Huang, and J. A. Rogers, Proc. Natl. Acad. Sci. USA **104**, 15607 (2007).
[5]H. Jiang, D.-Y. Khang, H. Fei, H. Kim, Y. Huang, J. Xiao, and J. A. Rogers, J. Mech. Phys. Solids **56**, 2585 (2008).
[6]T. Sekitani, H. Nakajima, H. Maeda, T. Fukushima, T. Aida, K. Hata, and T. Someya, Nat. Mater. **8**, 494 (2009).
[7]J. Xiao, A. Carlson, Z. J. Liu, Y. Huang, and J. A. Rogers, J. Appl. Mech.-Trans. ASME **77**, 011003 (2010).
[8]J. A. Rogers, T. Someya, and Y. Huang, Science **327**, 1603 (2010).
[9]Y. Huang, X. Wang, Y. Duan, N. Bu, and Z. Yin, Soft Matter **8**, 8302 (2012).
[10]S. Yang and N. Lu, Sensors **13**, 8577 (2013).
[11]R. H. Kim, D. H. Kim, J. Xiao, B. H. Kim, S. I. Park, B. Panilaitis, R. Ghaffari, J. Yao, M. Li, Z. Liu, V. Malyarchuk, D. G. Kim, A. P. Le, R. G. Nuzzo, D. L. Kaplan, F. G. Omenetto, Y. Huang, Z. Kang, and J. A. Rogers, Nat. Mater. **9**, 929 (2010).
[12]C. H. Lee, Y. J. Kim, Y. J. Hong, S. R. Jeon, S. Bae, B. H. Hong, and G. C. Yi, Adv. Mater. **23**, 4614 (2011).

[13]D. J. Lipomi, B. C. Tee, M. Vosgueritchian, and Z. Bao, Adv. Mater. **23**, 1771 (2011).
[14]E. C. Nelson, N. L. Dias, K. P. Bassett, S. N. Dunham, V. Verma, M. Miyake, P. Wiltzius, J. A. Rogers, J. J. Coleman, X. Li, and P. V. Braun, Nat. Mater. **10**, 676 (2011).
[15]H. C. Ko, M. P. Stoykovich, J. Song, V. Malyarchuk, W. M. Choi, C.-J. Yu, J. B. Geddes Iii, J. Xiao, S. Wang, Y. Huang, and J. A. Rogers, Nature **454**, 748 (2008).
[16]I. Jung, J. Xiao, V. Malyarchuk, C. Lu, M. Li, Z. Liu, J. Yoon, Y. Huang, and J. A. Rogers, Proc. Natl. Acad. Sci. USA **108**, 1788 (2011).
[17]Y. M. Song, Y. Xie, V. Malyarchuk, J. Xiao, I. Jung, K. J. Choi, Z. Liu, H. Park, C. Lu, R. H. Kim, R. Li, K. B. Crozier, Y. Huang, and J. A. Rogers, Nature **497**, 95 (2013).
[18]O. Graudejus, B. Morrison, C. Goletiani, Z. Yu, and S. Wagner, Adv. Funct. Mater. **22**, 640 (2012).
[19]D. P. J. Cotton, I. M. Graz, and S. P. Lacour, IEEE Sens. J. **9**, 2008 (2009).
[20]J. Viventi, D. H. Kim, J. D. Moss, Y. S. Kim, J. A. Blanco, N. Annetta, A. Hicks, J. Xiao, Y. Huang, D. J. Callans, J. A. Rogers, and B. Litt, Sci. Transl. Med. **2**, 24ra22 (2010).
[21]R. H. Kim, H. Tao, T. I. Kim, Y. Zhang, S. Kim, B. Panilaitis, M. Yang, D. H. Kim, Y. H. Jung, B. H. Kim, Y. Li, Y. Huang, F. G. Omenetto, and J. A. Rogers, Small **8**, 2812 (2012).
[22]S. Xu, Y. H. Zhang, L. Jia, K. E. Mathewson, K. I. Jang, J. Kim, H. R. Fu, X. Huang, P. Chava, R. H. Wang, S. Bhole, L. Z. Wang, Y. J. Na, Y. Guan, M. Flavin, Z. S. Han, Y. G. Huang, and J. A. Rogers, Science **344**, 70 (2014).
[23]D. H. Kim, N. S. Lu, R. Ma, Y. S. Kim, R. H. Kim, S. D. Wang, J. Wu, S. M. Won, H. Tao, A. Islam, K. J. Yu, T. I. Kim, R. Chowdhury, M. Ying, L. Z. Xu, M. Li, H. J. Chung, H. Keum, M. McCormick, P. Liu, Y. W. Zhang, F. G. Omenetto, Y. G. Huang, T. Coleman, and J. A. Rogers, Science **333**, 838 (2011).
[24]M. Kaltenbrunner, T. Sekitani, J. Reeder, T. Yokota, K. Kuribara, T. Tokuhara, M. Drack, R. Schwodiauer, I. Graz, S. Bauer-Gogonea, S. Bauer, and T. Someya, Nature **499**, 458 (2013).
[25]G. Schwartz, B. C. K. Tee, J. Mei, A. L. Appleton, D. H. Kim, H. Wang, and Z. Bao, Nat. Commun. **4**, 1859 (2013).
[26]L. Gao, Y. H. Zhang, V. Malyarchuk, L. Jia, K. I. Jang, R. C. Webb, H. R. Fu, Y. Shi, G. Y. Zhou, L. Shi, D. Shah, X. Huang, B. X. Xu, C. J. Yu, Y. Huang, and J. A. Rogers, Nat. Commun. **5**, 4938 (2014).
[27]S. Jung, J. Lee, T. Hyeon, M. Lee, and D. H. Kim, Adv. Mater. **26**, 6329 (2014).
[28]D. Son, J. Lee, S. Qiao, R. Ghaffari, J. Kim, J. E. Lee, C. Song, S. J. Kim, D. J. Lee, S. W. Jun, S. Yang, M. Park, J. Shin, K. Do, M. Lee, K. Kang, C. S. Hwang, N. S. Lu, T. Hyeon, and D. H. Kim, Nat. Nanotechnol. **9**, 397 (2014).
[29]T. Someya, T. Sekitani, S. Iba, Y. Kato, H. Kawaguchi, and T. Sakurai, Proc. Natl. Acad. Sci. USAe **101**, 9966 (2004).
[30]S. Wagner, S. P. Lacour, J. Jones, P.-h. I. Hsu, J. C. Sturm, T. Li, and Z. Suo, Physica E **25**, 326 (2004).
[31]S. C. Mannsfeld, B. C. Tee, R. M. Stoltenberg, C. V. Chen, S. Barman, B. V. Muir, A. N. Sokolov, C. Reese, and Z. Bao, Nat. Mater. **9**, 859 (2010).
[32]N. Lu, C. Lu, S. Yang, and J. Rogers, Adv. Funct. Mater. **22**, 4044 (2012).
[33]J. Kim, M. Lee, H. J. Shim, R. Ghaffari, H. R. Cho, D. Son, Y. H. Jung, M. Soh, C. Choi, S. Jung, K. Chu, D. Jeon, S. T. Lee, J. H. Kim, S. H. Choi, T. Hyeon, and D. H. Kim, Nat. Commun. **5**, 5747 (2014).
[34]D. H. Kim, J. Song, W. M. Choi, H. S. Kim, R. H. Kim, Z. Liu, Y. Y. Huang, K. C. Hwang, Y. W. Zhang, and J. A. Rogers, Proc. Natl. Acad. Sci. USA **105**, 18675 (2008).
[35]D. H. Kim, Z. Liu, Y. S. Kim, J. Wu, J. Song, H. S. Kim, Y. Huang, K. C. Hwang, Y. Zhang, and J. A. Rogers, Small **5**, 2841 (2009).
[36]J. Lee, J. Wu, M. Shi, J. Yoon, S. I. Park, M. Li, Z. Liu, Y. Huang, and J. A. Rogers, Adv. Mater. **23**, 986 (2011).
[37]S. Xu, Y. H. Zhang, J. Cho, J. Lee, X. Huang, L. Jia, J. A. Fan, Y. W. Su, J. Su, H. G. Zhang, H. Y. Cheng, B. W. Lu, C. J. Yu, C. Chuang, T. I. Kim, T. Song, K. Shigeta, S. Kang, C. Dagdeviren, I. Petrov, P. V. Braun, Y. Huang, U. Paik, and J. A. Rogers, Nat. Commun. **4**, 1543 (2013).
[38]J. Song, Y. Huang, J. Xiao, S. Wang, K. C. Hwang, H. C. Ko, D. H. Kim, M. P. Stoykovich, and J. A. Rogers, J. Appl. Phys. **105**, 123516 (2009).
[39]Y. W. Su, J. Wu, Z. C. Fan, K. C. Hwang, J. Z. Song, Y. G. Huang, and J. A. Rogers, J. Mech. Phys. Solids **60**, 487 (2012).
[40]Y. H. Zhang, S. Xu, H. R. Fu, J. Lee, J. Su, K. C. Hwang, J. A. Rogers, and Y. Huang, Soft Matter **9**, 8062 (2013).
[41]Y. H. Zhang, H. R. Fu, S. Xu, J. A. Fan, K. C. Hwang, J. Q. Jiang, J. A. Rogers, and Y. Huang, J. Mech. Phys. Solids **72**, 115 (2014).
[42]T. Li, Z. G. Suo, S. P. Lacour, and S. Wagner, J. Mater. Res. **20**, 3274 (2005).
[43]Y. H. Zhang, S. D. Wang, X. T. Li, J. A. Fan, S. Xu, Y. M. Song, K. J. Choi, W. H. Yeo, W. Lee, S. N. Nazaar, B. W. Lu, L. Yin, K. C. Hwang, J. A. Rogers, and Y. Huang, Adv. Funct. Mater. **24**, 2028 (2014).
[44]M. Gonzalez, F. Axisa, M. V. BuIcke, D. Brosteaux, B. Vandevelde, and J. Vanfleteren, Microelectron. Reliab. **48**, 825 (2008).
[45]Y. Y. Hsu, M. Gonzalez, F. Bossuyt, F. Axisa, J. Vanfleteren, and I. De Wolf, J. Mater. Res. **24**, 3573 (2009).
[46]S. Yang, B. Su, G. Bitar, and N. Lu, Int. J. Fracture **190**, 99 (2014).